Slc26a3/Dra and Slc26a6 in Murine Ameloblasts

Journal of Dental Research
2015, Vol. 94(12) 1732–1739
© International & American Associations for Dental Research 2015
Reprints and permissions:
sagepub.com/journalsPermissions.nav
DOI: 10.1177/0022034515606873
jdr.sagepub.com

R. Jalali[1], B. Zandieh-Doulabi[1], P.K. DenBesten[2], U. Seidler[3], B. Riederer[3], S. Wedenoja[4], D. Micha[5], and A.L.J.J. Bronckers[1]

Abstract

Formation of apatite crystals during enamel development generates protons. To sustain mineral accretion, maturation ameloblasts need to buffer these protons. The presence of cytosolic carbonic anhydrases, the basolateral Na^+ bicarbonate cotransporter Nbce1, and the basolateral anion exchanger Ae2a,b in maturation ameloblasts suggests that these cells secrete bicarbonates into the forming enamel, but it is unknown by which mechanism. Solute carrier (Slc) family 26A encodes different anion exchangers that exchange Cl^-/HCO_3^-, including Slc26a3/Dra, Slc26a6/Pat-1, and Slc26a4/pendrin. Previously, we showed that pendrin is expressed in ameloblasts but is not critical for enamel formation. In this study, we tested the hypothesis that maturation ameloblasts express Dra and Slc26a6 to secrete bicarbonate into the enamel space in exchange for Cl^-. Real-time polymerase chain reaction detected mRNA transcripts for *Dra* and *Slc26a6* in mouse incisor enamel organs, and Western blotting confirmed their translation into protein. Both isoforms were immunolocalized in ameloblasts, principally at maturation stage. Mice with null mutation of either *Dra* or *Slc26a6* had a normal dental or skeletal phenotype without changes in mineral density, as measured by micro–computed tomography. In enamel organs of *Slc26a6*-null mice, Dra and pendrin protein levels were both elevated by 52% and 55%, respectively. The amount of Slc26a6 protein was unchanged in enamel organs of *Ae2a,b*- and *Cftr*-null mice but reduced in *Dra*-null mice by 36%. Our data show that ameloblasts express *Dra, pendrin*, or *Slc26a6* but each of these separately is not critical for formation of dental enamel. The data suggest that in ameloblasts, Slc26a isoforms can functionally compensate for one another.

Keywords: enamel organ, micro–computed tomography, immunolocalization, *Dra*-null mice, *Slc26a6*-null mice, mineralization

Introduction

Ameloblasts form enamel in 2 stages: a secretion stage, in which they secrete a protein-rich matrix primarily consisting of amelogenins, and a maturation stage, during which most of these proteins are degraded and removed from the enamel space. Simultaneously, mineral is deposited in an ordered pattern. Formation of apatite mineral releases protons into the enamel matrix microenvironment, which could acidify the enamel compartment (Lacruz, Nanci, Kurtz, et al. 2010; Lacruz et al. 2012). During the secretory stage, mineral accretion is low, and the pH may in part be regulated by amelogenins, shown to have a high buffering capacity (Ryu et al. 1996; Guo et al. 2015). During maturation, however, the rate of mineral formation increases (Smith et al. 2005), and removal of amelogenins from the enamel compartment implies the necessity for enamel matrix pH to be regulated by other mechanisms. Various studies support the idea that ameloblasts secrete bicarbonate into the enamel space via transmembrane proteins (Smith 1998). Hypomineralization of dental enamel and changes in the structure of enamel seen in mice with defective or dysfunctional cystic fibrosis transmembrane conductance regulator (Cftr; Wright et al. 1996), basolateral anion exchanger 2 (Ae2; Lyaruu et al. 2008), and Na^+ bicarbonate cotransporter Nbce1 (Gawenis et al. 2005; Jalali et al. 2014) support the concept that ameloblasts are involved in secreting bicarbonates (Lacruz, Nanci, White, et al. 2010). The molecular mechanisms responsible for actually secreting bicarbonate into the enamel space is unknown, but it likely is an anion exchanger located in the apical membrane facing the forming enamel.

[1]Department of Oral Cell Biology, Academic Centre for Dentistry Amsterdam, University of Amsterdam, and MOVE Research Institute, VU University Amsterdam, Amsterdam, Netherlands
[2]Department of Oral Sciences, University of California, San Francisco, CA, USA
[3]Abteilung Gastroenterologie, Hepatologie und Endokrinologie, Medizinische Hochschule Hannover, Hannover, Germany
[4]Department of Medical Genetics, Biomedicum Helsinki, University of Helsinki, Finland
[5]Department of Clinical Genetics, Vrije Universiteit Medical Center, Amsterdam, Netherlands

A supplemental appendix to this article is published electronically only at http://jdr.sagepub.com/supplemental.

Corresponding Author:
A.L.J.J. Bronckers, Department of Oral Cell Biology, ACTA, Gustav Mahlerlaan 3004, 1081 LA, Amsterdam, The Netherlands.
Email: a.bronckers@acta.nl

The solute carrier (SLC) gene family comprises ~55 gene families that contain ~360 protein-coding genes (Alper et al. 2013), several of which have been detected in ameloblasts (Gawenis et al. 2005; Lyaruu et al. 2008; Paine et al. 2008; Bronckers et al. 2010; Josephsen et al. 2010; Lacruz, Nanci, Kurtz, et al. 2010; Bronckers et al. 2011; Bronckers et al. 2012). Previous studies have shown that in other epithelial cells, the chloride channel Cftr is functionally involved in pH regulation. Mutation of Cftr affects many cell types, including sweat glands, intestine, bile ducts, pancreatic ducts, respiratory epithelia, submandibular glands, uterus, and vas deferens (Trezise et al. 1991; Tizzano et al. 1993; Zeng et al. 1997; Claass et al. 2000). These studies suggested 2 possible functions for CFTR: transport of Cl^- and regulation of the activity of other Cl^-/HCO_3^- transporters (Ko et al. 2002; Steward and Ishiguro 2009). Therefore, by conducing Cl^- imported from interstitial tissue fluid by basolateral Ae2 in exchange for intracellular bicarbonate (Wright et al. 1996; Arquitt et al. 2002; Bronckers et al. 2010; Lacruz et al. 2012), Cftr provides the enamel space with Cl^- that can be exchanged for bicarbonates mediated by anion exchangers in the apical membranes. The SLC family A26 (SLC26A) encodes multifunctional anion exchangers that transport a wide range of substrates, including Cl^-, HCO_3^-, sulfate, oxalate, and formate (Soleimani and Xu 2006).

SLC26A members that exchange Cl^-/HCO_3^- include SLC26A3/DRA (downregulated in adenoma), SLC26A4 (pendrin), and SLC26A6 (putative anion transporter 1; Soleimani and Xu 2006). The mouse Dra protein consists of 575 amino acids, whereas Slc26a4 and Slc26a6 are each 780 amino acids long (86 kDa). Slc26a4 is predominantly expressed in the thyroid, inner ear, and kidney (Wall et al. 2003); Slc26a6, in both kidney and the gastrointestinal tract (Lohi et al. 2000; Sindic et al. 2007); and Dra, in the mucosa of the lower intestinal tract, apical membranes of columnar epithelium, and pancreatic ducts (Lamprecht et al. 2009). Homozygous mutations in *DRA* cause congenital chloride diarrhea (Höglund et al. 1996), whereas mutation in *SLC26A6* causes hyperoxaluria, hyperoxalemia, and calcium oxalate urolithiasis (Jiang et al. 2006).

We showed that secretory- and maturation-stage mouse ameloblasts express Slc26a4 (pendrin). However, disruption of this gene presented no dental phenotype possibly by compensation by other Slc26a members (Bronckers et al. 2011). Ameloblasts resemble pancreatic ductal epithelium that expresses various Slc26a members (Dra and Slc26a6) to secrete bicarbonates (Steward and Ishiguro 2009). In this study we addressed 2 questions: (1) Do mouse ameloblasts express Dra and Slc26a6? (2) Is there compensation between different Slc26a family members that could explain why pendrin-null mice, for example, have no dental phenotype?

To test this, the enamel organs of mice were analyzed for expression of Dra and Slc26a6 at the protein level. The effect of the null mutation of both isoforms on enamel development and their potential compensation by changes in Dra and Slc26a6 expression was studied by micro–computed tomography and Western blotting in *Dra*- and *Slc26a6*-null mice. In various types of transport epithelia, the transport activity of Slc26A isotypes depends on functional Cftr, so we also determined whether the amount of Slc26a6 protein was changed in *Cftr*-null ameloblast.

Material and Methods

Animals

Tissues were collected from adult *Dra*-null mice (129S6/SvEv mouse strain; Xia et al. 2014) and *Slc26a6*-null mice (strain of 129/SvJ mouse phage library kindly donated by Dr. P. Aronson, Yale University, New Haven, CT, USA; Jiang et al. 2006) and wild-type control littermates. After sacrifice, lower jaws and several other soft tissues were excised, slam-frozen and freeze-dried, or fixed for immunohistochemistry according to a standard protocol and shipped to Amsterdam for processing and analysis. Details on these mutant mice have been published elsewhere (Jiang et al. 2006; Xia et al. 2014). Briefly, *Slc26a6*-null mutant mice were generated by replacing exons 1 and 2 and part of exon 3 in the *Slc26a6* gene by a Neo gene cassette. *Dra*-null mice were generated by inserting a Neo cassette into exon 2 of the *Dra* gene. Mouse enamel organs with a null mutation in *Ae2a,b* and *Cftr* and 6- to 8-d-old wild-type mice were from previous studies (Lyaruu et al. 2008; Bronckers et al. 2010). All animal handling complied with national and international regulations for animal care, and permission was obtained from the Committee for Animal Care of Abteilung Gastroenterologie, Medizinische Hochschule Hannover (Hannover, Germany), and Department of Medicine, University of Yale (New Haven, CT, USA).

Histologic Procedures

For immunohistochemistry, tissues from *Slc26a6*-null, *Dra*-null, and control mice ($n = 3$ in each) were fixed in 4% formaldehyde in 0.1M phosphate buffer at pH 7.4 overnight, decalcified in 10% EDTA containing 0.8% formaldehyde at pH 7.4 for 6 wk at room temperature, embedded in paraffin, and sectioned. Mandibles from *Slc26a3/Dra*- and *Slc26a6*-null mice and wild-type littermates were scanned by micro–computed tomography prior to decalcification.

Real-time Quantitative Polymerase Chain Reaction

Total RNA was extracted from tissues with the NucleoSpin RNA/Protein Kit (Macherey-Nagel, Düren, Germany) according to the manufacturer's instructions. First-strand cDNA synthesis was performed in a 20-µL reverse transcription (RT) reaction containing 200 ng of total RNA via the VILO Kit (Invitrogen, Bleiswijk, Netherlands) according to the manufacturer's instructions. Real-time polymerase chain reaction (PCR) analysis was used to analyze mRNA expression of *Dra* and *Slc26a6* and the housekeeping protein tyrosine 3-monooxygenase (YWHAZ) with the primer sequences shown in the Appendix Table by using the LightCycler 480 system based on SYBR Green I dye (Roche Applied Science, Indianapolis, IN, USA). The LightCycler reactions were prepared in 20 µL of total

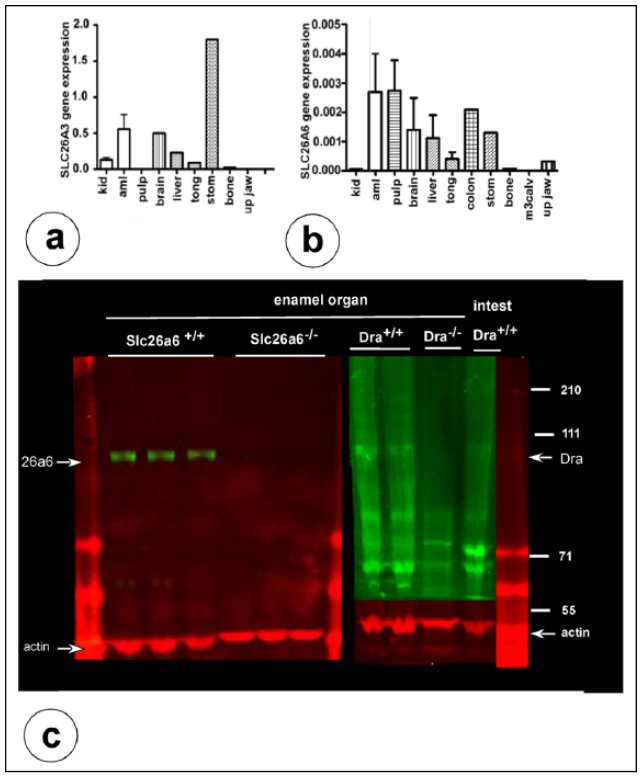

Figure 1. Gene and protein expression for *Dra* and *Slc26a6* in mouse enamel organs. Real-time polymerase chain reaction of mouse wild-type tissues for *Dra* (**a**) and *Slc26a6* (**b**) transcripts. The values on the *y*-axis represent fold difference for the relative mRNA expression (normalized by the housekeeping protein ywhaz; in various tissues. Aml, enamel organ; kid, kidney; m3calv, MC3T3 mouse calvarial osteoblast-like cells; stom, stomach. (**c**) Western blots of enamel organ extracts from wild-type/$Dra^{+/+}$ and *Dra*-null mice stained with anti-Dra (right arrow) and *Slc26a6*-null mice stained with anti-Slc26a6 (left arrow). The 43-kDa bands are positive with anti-actin.

volume with 7 µL of PCR-H_2O, 0.5 µL of forward primer (0.2 µM), 0.5 µL of reverse primer (0.2 µM), 10 µL of LightCycler Mastermix (LightCycler 480 SYBR Green I Master; Roche Applied Science), to which 2 µL of cDNA (5 times diluted) was added as PCR template. Controls in the real-time RT PCR reaction included RT reactions without the reverse transcriptase (control for DNA carryover) and RT reactions without template (control for reagent contamination). With the LightCycler software, the crossing points were assessed from a standard curve of 5 serial dilutions ranging from 10 ng to 1.6 pg of cDNA. PCR efficiency (E) was automatically calculated with the fit point method (E = 10–1/slope). Gene expression data were used only if the PCR E was within a range of 1.85 to 2.0. From each gene, the amount of measured DNA was normalized to that of the YWHAZ housekeeping gene to calculate relative gene expression.

Immunohistochemical Staining

Paraffin sections were dewaxed in xylene, rehydrated in a descending series of ethanol, and rinsed in phosphate-buffered saline (PBS). The following antisera were used:

1) mouse monoclonal anti-Dra (H0001811-M01; Abnova, Taipei, Taiwan) against a peptide corresponding with amino acid sequence 503 to 600 of mouse Dra (TQFP KCSTLANIGRTNIYKNKKDYYDMYEPEGVKIF RCP-SPIYFANIGFFRRKLIDAVGFSPLRILRKRN KALRKIR KLQKQGLLQVTPKGFICTVDT);
2) rabbit anti-Dra (Research Genetics, Huntsville, AL, USA) against the synthetic peptide FNPSQEKDGKIDF, corresponding to amino acids 731 to 744 of the human SLC26A3/DRA cDNA (GenBank L02785.1)—this antiserum was further purified on a protein G minicolumn;
3) affinity-purified rabbit anti-Slc26a6 against a peptide (DLRRRDYHMERPLLNQEHLEE) of the N-terminal domain (amino acids 23–43) of human SLC26A (donated by Dr. P. Aronson, Yale University, New Haven, CT, USA; and
4) affinity-purified rabbit anti-pendrin (Slc26a4; SC-50346, H-195; Santa Cruz Biotechnology, Tebu-Bio, Heerhugowaard, Netherlands; Bronckers et al. 2011; Bronckers et al. 2012).

Antigen retrieval was performed either in 10mM citrate buffer (pH 6.0) at 60 °C overnight or for 20 min in a microwave at 95 °C prior to staining or by a mild predigestion with a proteinase K solution (10 µg/mL; in PBS) for 15 min at 37 °C. After retrieval, endogenous peroxidase was inactivated with a peroxidase block solution (EnVision Kit; DakoCytomation, Carpinteria, CA, USA) for 5 min. Sections were washed in 0.1M TBS (Tris-buffered saline; 0.9% NaCl, pH 7.2) containing 0.1% bovine serum albumin. To prevent nonspecific staining, sections were incubated for 30 min with 2% bovine serum albumin in PBS. Sections were then incubated overnight at 4 °C with primary antibodies or with matched nonimmune IgG (1 to 2 µg/mL) or normal serum (1:100 to 1:200) to serve as controls. Prior to incubation of mouse tissues with primary mouse antibodies, sections were incubated with mouse-on-mouse blocking kit (HistoMouse BEAT Blocker Kit; Invitrogen). After overnight incubation at 4 °C with primary antibodies, sections were washed 3 times in TBS and incubated 1) with goat-antirabbit IgG antibodies conjugated with peroxidase polymer or rabbit antimouse IgG conjugated with peroxidase polymer (EnVision Kits) for 1 h at room temperature and counterstained with hematoxylin or 2) with goat antirabbit–Alexa Fluor 488 (5 µg/mL; Invitrogen) 1 to 2 h at room temperature and counterstained with DAPI (Vector Laboratories, Burlingame, CA, USA).

Western Blotting

From freeze-dried mandibular incisors, enamel organs at early maturation stage from wild-type and null mutant mice were microdissected incisally from a reference line projected between M1 and M2 to make a distinction between secretory and maturation stages. The apical half of the enamel organ was dissected, dissolved under nonreducing condition in SDS loading buffer (NucleoSpin TriPrep; Macherey-Nagel, Bioke, Leiden, The Netherlands), and protein was measured with the BCA protein assay (Bio-Rad, Hercules, CA, USA). Five to

10 µg of kidney and colon denatured protein or 20 to 30 µg of enamel organ denatured protein were loaded on SDS-PAGE in a 3% to 8% Tris acetate NuPAGE gel (Thermo Fisher Scientific, Grand Island, NY, USA) with Tris acetate as running buffer for 60 min at 150 V and electroblotted by an iBlot device (Invitrogen) on nitrocellulose membrane according to the manufacturer's instructions. Blots were incubated with rabbit primary antibodies (1:200 antibodies) and mouse-β-actin antibody (1:1,000; Sigma-Aldrich, St. Louis, MO, USA) overnight. IRDye 800CW conjugated goat anti-rabbit IgG (H+L) highly cross-adsorbed (926-32211; LI-COR Biosciences, Lincoln, NE, USA) and IRDye 680CW conjugated goat anti-mouse IgG (H+L) highly cross-adsorbed (926-32220; LI-COR) were applied as a second antibody for 90 min at room temperature (1:5,000; LI-COR) prior to washing with PBS. Visualization and quantification were carried out with the OdysseyH scanner and software (LI-COR). Red color (for actin) was detected at a 680-nm wavelength, and a green color (Slc26A members) was detected at a 800-nm wavelength. For quantification, Odyssey software was used. Intensity values of the bands were normalized for actin and expressed as percentage of wild type (100%).

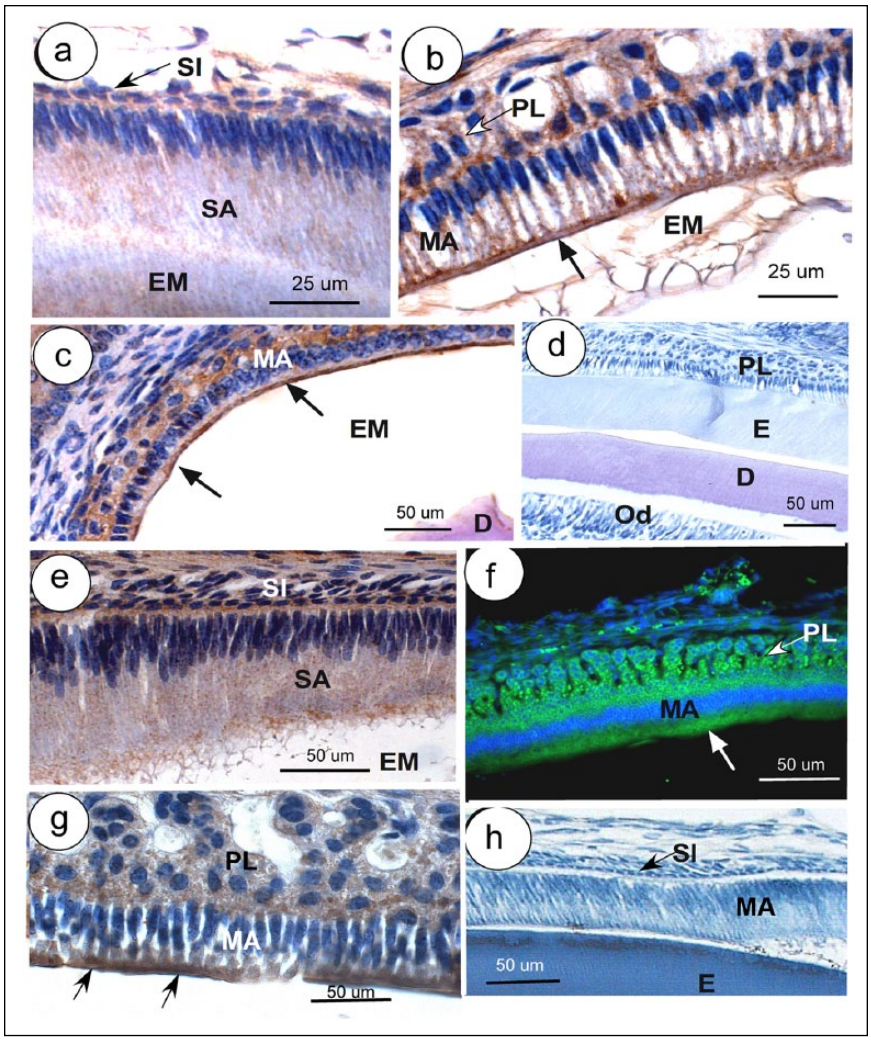

Figure 2. Immunolocalization of Dra (**a–d**) and Slc26a6 (**e–g**) in developing mouse teeth. Secretory ameloblasts (SA; a) and maturation ameloblasts (MA; b, c) are positive for Dra, particularly the apical parts (arrows; b, c); some staining is also presents in papillary layer (PL; b, c). (d) A *Dra*-null incisor stained with anti-Dra. (e) Weak staining for Slc26a6 is seen in late SA, strong staining in MA and PL (f, g). (f, g) Arrows indicate apical staining. (h) Part of an incisor of a wild-type mouse in which anti-Slc26a6 was replaced by nonimmune IgG. Except for panel c (developing molar), all sections were taken from incisors. (f) Immunofluorescent staining (green); all other figures, peroxidase staining (brown). D, dentin; E, enamel; EM, enamel matrix; ES, enamel space; Od, odontoblasts; SI, stratum intermedium (arrows in panels a and h); ST, stratum intermedium. This figure is available in color online at http://jdr.sagepub.com.

Micro–computed tomography

To determine mineral density, hemimandibles from 16-wk-old mouse mutants and littermate wild-type controls were scanned at 55 kV, 145-µA beam intensity, 8-µm image pixel size, with a µCT-40 high-resolution scanner (Scanco Medical AG, Bassersdorf, Switzerland). Mineral density was determined at sequential stages of development. An internal standard made of solid-sintered apatite (5-mm diameter, 1.5 to 2.0 mm thick, solid sintered) with density of 2.9 ± 0.2 g/mL (a gift from Himed; http://www.himed.com) was used as high-density standard. Cross-sectional virtual images were collected from the most developed (incisor tip) to the least developed (cervical area; Fig. 4a). The slice at the incisor tip containing the most highly mineralized enamel was identified visually. Measurements in enamel were made halfway between enamel surface and enamel-dentin junction at 500-µm intervals (50 slices at 10-µm interval), at 3 sites per slice, averaged, and calculated per developmental stage per mouse. Group averages (3 mice/group) were calculated and plotted as function of stage (slice number). Independent *t* test was used to compare the groups. Statistical significance was set at $P < 0.05$.

Results

Real-time Quantitative PCR

PCR analysis based on mouse-specific primers confirmed that mRNA transcripts for *Dra* were detectable in enamel organ, liver, brain, and stomach (Fig. 1a). Transcripts for *Slc26a6* were detectable in enamel organs, dental pulp, brain, liver, tongue, colon, and stomach (Fig. 1b).

Immunodetection and Immunolocalization of Slc26a3/Dra and Slc26a6 in Developing Teeth

On Western blots, characteristic bands between 70 and 110 kDa immunoreactive with anti-Dra and anti-Slc26a6 were identified in enamel organ extracts of wild-type mice. Failure

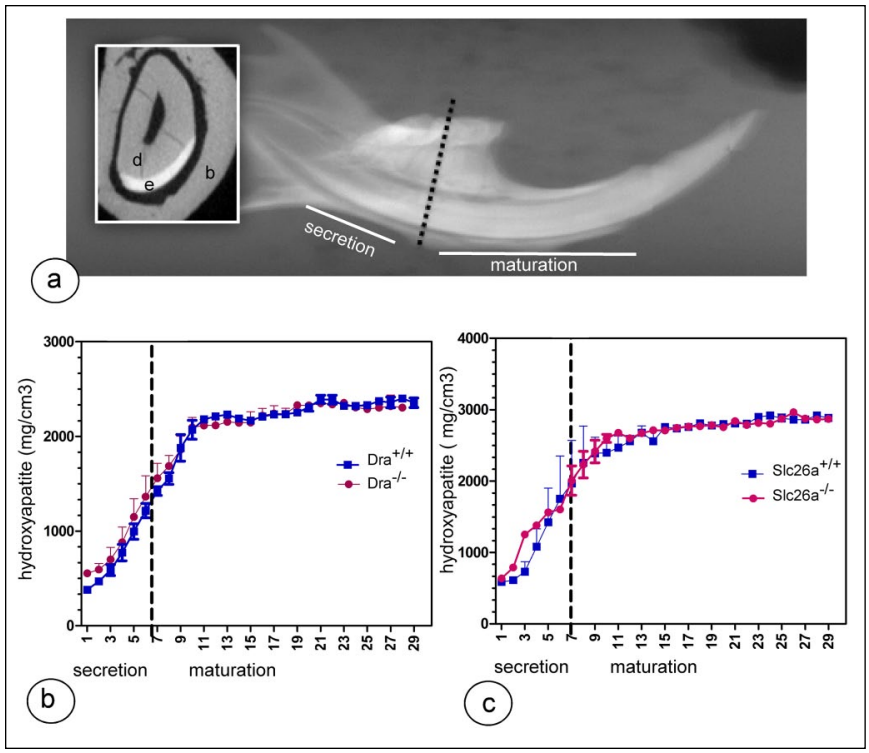

Figure 3. The mineral density of lower incisor enamel. (**a**) Broken line indicates the reference line between first and second molars indicating the approximate transition from secretory stage to maturation stage (inset: cross section; b, bone; d, dentin; e, enamel) from a wild-type mouse. (**b**, **c**) *Dra*- and *Slc26a6*-null mutant mice show mineral density measurements plotted against slice numbers (representing progressive stages of enamel formation with 500-µm intervals). The mineral content of both null mutant mice (red) is not different from that of wild-type littermate controls (blue). This figure is available in color online at http://jdr.sagepub.com.

to stain these bands in *Dra*- and *Slc26a6*-null tissue validated the specificity of the antibodies (Fig. 1c)

Weak fine-granular intracellular staining for Dra was noted in secretory ameloblasts (Fig. 2a), as well as strong intracellular staining with preference over the apical membranes in maturation ameloblasts (Fig. 2b, c). Ameloblasts of *Dra*-null and *Slc26a6*-null mice did not stain with their respective antibodies (only shown for *Dra*-null ameloblasts) (Fig. 2d).

Staining for Slc26a6 was granular and weak in the secretory stage, increased at late secretory stage (Fig. 2e), and strong in the maturation-stage ameloblasts (Fig. 2f) concentrating apically (Fig. 2g). The papillary layer was positive in early and midmaturation, but staining was low at late maturation stage (Fig. 2f, g). When primary antibodies were replaced by nonimmune serum or matching nonimmune IgG, cells did not stain (Fig. 2h), except occasionally over extracellular matrices, especially in undecalcified sections or tissues that were incompletely decalcified.

Analysis of Enamel Formation in Dra- *and* Slc26a6-*null Mice*

No anatomic changes were observed in incisors or molars of *Dra*- and *Slc26a6*-null mice; incisors had the usual orange pigment, contained a sharp edge, and showed no excessive wear.

Micro–computed tomography analysis showed that the mineral density in both mutant strains was not different from their wild-type littermate controls (Fig. 3). Histologic evaluation showed no apparent changes in ameloblast or enamel structure in mutant mice.

Changes in Protein Levels for Slc26a Isoforms in Dra- *and* Slc26a6-*null Ameloblasts*

To examine whether in ameloblasts the members of Slc26a family could compensate for one another, we tested maturation-stage enamel organs from null mutant tissues for changes of expression of the nonmutated isoforms by Western blotting (Fig. 4).

Maturation-stage ameloblasts from *Dra*-null mice stained with anti-Slc26a6 (Fig. 4) showed a 36% decrease of staining intensity compared with wild-type littermate controls ($P = 0.015$). In *Slc26a6*-null mice, staining for Dra and pendrin/Slc26a4 had increased by 52% ($P = 0.01$) and 55% ($P = 0.002$), respectively. Enamel organs of *Ae2a,b*-null mice stained for Dra (Fig. 4), and Slc26a6 showed no quantitative change in protein expression. In *Cftr*-null ameloblasts, Slc26a6 protein tended to be enhanced, but this was not statistically significant (Fig. 4; $P = 0.10$).

Discussion

In the present study, we examined the expression by, and the potential role of, Dra and Slc26a6 in ameloblasts during formation of dental enamel. We detected immunoreactive protein bands of the predicted sizes for both transporters in enamel organs of wild-type mice but not in enamel organs of null-mutant mice. We found that the apical border of maturation ameloblasts stained positive with anti-Slc26a6 and anti-Dra, as found for pendrin (Bronckers et al. 2011) and Cftr (Bronckers et al. 2010). These results show that maturation ameloblasts express all 3 Slc26a isoforms in the same membrane domain as Cftr (i.e., the apical plasma membrane, facing forming enamel; Fig. 5). This distribution pattern resembled that in pancreatic tubular epithelium, cells that secrete large amounts of bicarbonates to neutralize acid gastric juice (Steward and Ishiguro 2009). Absence of Slc26a or Dra did not affect enamel structure or mineral density, indicating that each of these exchangers expressed alone is not critical for enamel formation. Loss of Slc26a6 resulted in enhanced levels of Dra and pendrin protein, suggesting that ameloblasts compensate the loss of Slc26a by producing more Dra and pendrin. In pancreatic ductal epithelium, the stoichiometry of Cl^-/HCO_3^- exchange differs for the various Slc26A isoforms: for pendrin, the stoichiometry for $Cl^-:HCO_3^-$ is 1:1 (electroneutral); for Slc26A6, 1:2; and for Dra, 2:1 (Ko et al. 2002; Steward and Ishiguro 2009). In native pancreatic mouse ducts, null mutation of apical *Slc26a6*

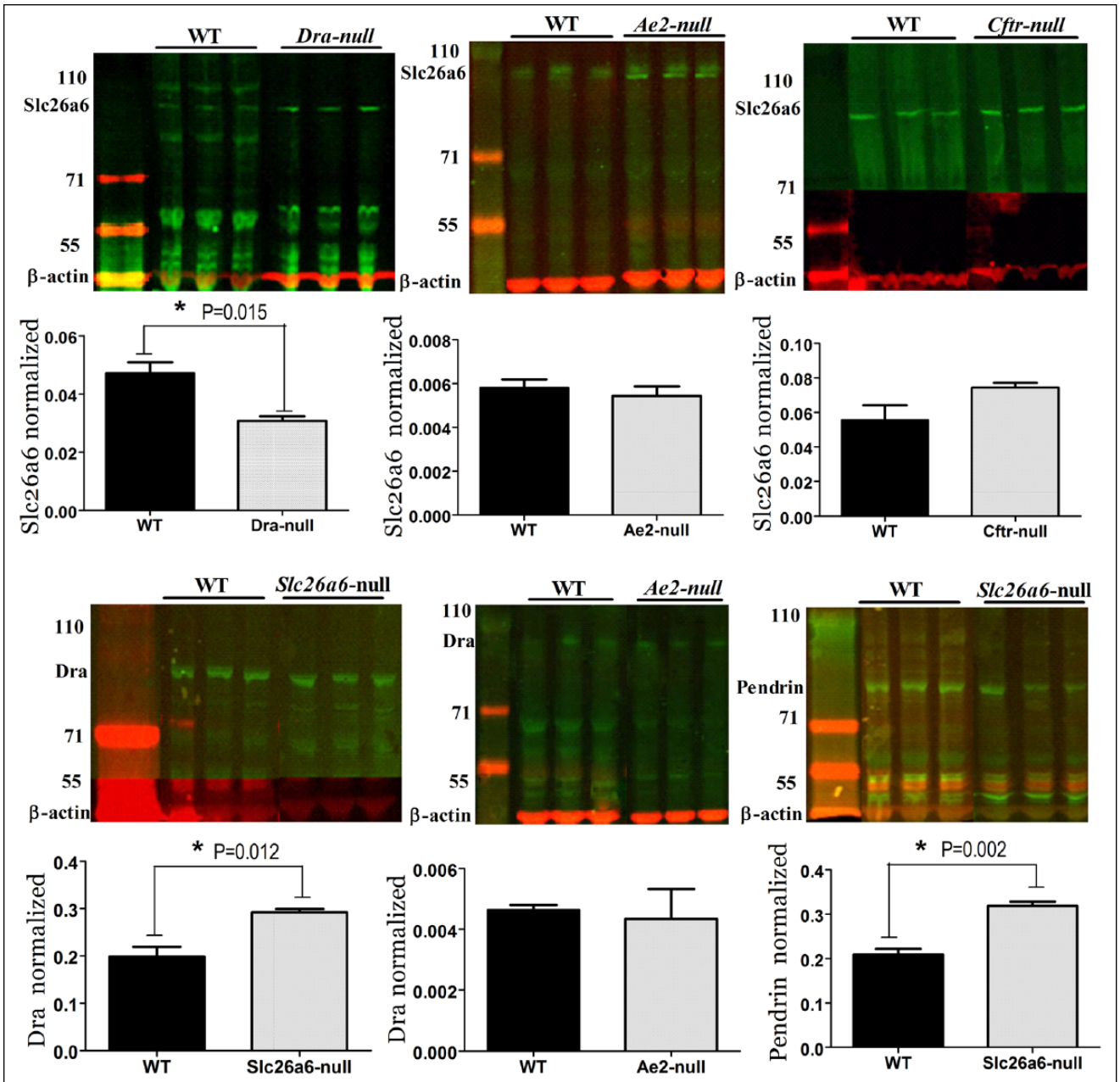

Western blot probed with	Enamel organ Genotype			
	***Slc26a6*-null**	***Dra*-null**	***Ae2*-null**	***Cftr*-null**
Anti-SLC26A6	Negative	-36%*	No change	No change
Anti-DRA	+52%*	Negative	No change	-
Anti-PENDRIN	+55%*	-	-	-

Figure 4. Western blots of enamel organ extracts from *Slc26a*-null mice stained with anti-Dra, anti-Slc26a6, or anti-pendrin to detect up- or downregulation of isoforms of the Slc26a family. Top row from left to right: enamel organ extracts from *Dra*-, Ae2-, and *Cftr*-null mice stained with anti-Slc26a6. The bar graphs in the second row represent the density measurements. Third row: extracts from *Slc26a6*-, Ae2-, and *Slc26a6*-null mice stained with anti-Dra (*Slc26a6* and Ae2) or anti-pendrin. Fourth row represents density measurements. The table at the bottom presents a summary of the changes. WT, wild type.

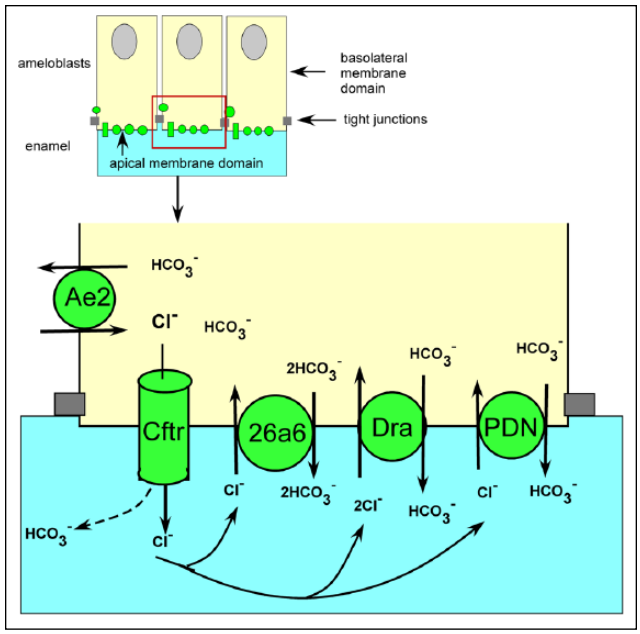

Figure 5. Potential role of Slc26a isotypes during maturation-stage amelogenesis. To neutralize protons released during apatite formation in the enamel space (light blue), the members of Slc26a family secrete bicarbonates in exchange for Cl^-. Basolateral anion exchanger 2 (Ae2) imports Cl^- from the extracellular tissue fluid in exchange for bicarbonate. Cl^- is conduced through Cftr into the enamel, from which it is exchanged back against bicarbonate by Slc26a isotypes. Null mutation of *Slc26a6* is compensated by upregulation of pendrin and *Dra*, which requires more Cl^- to transport bicarbonate. Null mutation of *Dra* may change the membrane potential, leading to a drop in activity and in the amount of Slc26a6 protein. Cftr can also conduce bicarbonate up to 25% of its capacity, and can transduce bicarbonate up to 100% of its capacity (Park et al. 2010). This figure is available in color online at http://jdr.sagepub.com.

blocked the secretion of bicarbonate and upregulated transport activity across the apical membranes of an exchanger mediating 2:1 exchange, most probably Dra (Song et al. 2012). If the same stoichiometry for Cl^-/bicarbonate exchange holds for ameloblast as for pancreatic tubular epithelium, similar changes may occur in ameloblasts (Fig. 5). Slc26a6 would secrete 2 bicarbonates in exchange for 1 Cl^-, overall 1 more negative charge than it imports. This would result into intracellular alkalinization and affect the membrane potential, which is compensated by higher Dra and pendrin activity.

The absence of Dra in ameloblasts, however, may result into an increase of the intracellular steady-state intracellular pH (as in intestine [Xia et al. 2014] but perhaps different in pancreas), which is counteracted by lowering Slc26a6 protein to reduce the driving force for bicarbonate secretion. Functional studies measuring pH and transport of Cl^- are required to test secretion of these ions across the ameloblast layer.

With respect to the small changes in protein levels of Slc26a isotypes in null mutation of Dra or Slc26a, in pancreatic and salivary ductal epithelium and HEK 293 cells, Cftr plays a role either by transducing bicarbonate by itself (Fig. 5; Park et al. 2010) or by stimulating transport activity of DRA, SLC26A6, and PENDRIN as much as 5- to 6-fold without changing the protein levels of these exchangers (Ko et al. 2002; Ko et al. 2004). Even small changes in protein levels of Slc26a isoforms in mouse ameloblasts could strongly enhance their transport activity to compensate loss of Slc26a6. The absence of a dental phenotype in *Dra-, Slc26a6-*, and *pendrin*-null mice could also be due to compensation by other Slc26a members (Slc26a7, 26a9, or 26a11) all capable of exchanging bicarbonate and Cl^- . Mouse embryos with a double knockout for *Dra* and *Slc26a6* are not viable and die intrauterine (unpublished results by U.S.). Further studies are needed using tissue-specific or inducible inactivation of combinations of various Slc26a isoforms to disclose their function in ameloblasts.

In conclusion, the individual inactivation of the Slc26a isoforms does not induce structural changes or mineralization defects in forming enamel. Upregulation of Dra and Slc26a6 protein in Slc26a6-deficient ameloblasts suggests that Slc26a members can compensate for one another.

Author Contributions

R. Jalali, A.L.J.J. Bronckers, contributed to conception, design, data acquisition, and analysis, drafted and critically revised the manuscript; B. Zandieh-Doulabi, S. Wedenoja, D. Micha, contributed to data acquisition and analysis, critically revised the manuscript; P.K. DenBesten, contributed to design, data acquisition, analysis, and interpretation, critically revised the manuscript; U. Seidler, contributed to data acquisition, analysis, and interpretation, critically revised the manuscript; B. Riederer, contributed to data acquisition, critically revised the manuscript. All authors gave final approval and agree to be accountable for all aspects of the work.

Acknowledgments

This study was supported by the National Institutes of Health (DE13508; to Drs. P. DenBesten, A. Bronckers, and D. Lyaruu). We thank Mr. T.J.M. Bervoets, Dr. L. van Ruijven (ACTA, Amsterdam, Netherlands), and Dr. Zhenglin Yuan (Medizinische Hochschule Hannover, Hannover, Germany) for their expert technical help; Dr. M.J. Bijvelds (Erasmus University, Rotterdam, Netherlands) for providing *Cftr*-null tissues; Drs. J. Medina and S. Sarvide (University of Navarra, Pamplona, Spain) for *Ae2*-null tissues; and Drs P. Aronson and Z. Jia (University of Yale, New Haven, CT, USA) for providing *Slc26a6*-null tissues and anti-Slc26a6 antibody. The authors declare no potential conflicts of interest with respect to the authorship and/or publication of this article.

References

Alper SL, Sharma AK. 2013. The SLC26 gene family of anion transporters and channels. Mol Aspects Med. 34(2–3):494–515.

Arquitt CK, Boyd C, Wright JT. 2002. Cystic fibrosis transmembrane regulator gene (CFTR) is associated with abnormal enamel formation. J Dent Res. 81(7):492–496.

Bronckers AL, Guo J, Lyaruu DM, DenBesten PK, Zandieh-Doulabi B. 2012. Immunolocalization and western blotting of the anion exchanger pendrin in ameloblasts. Eur J Oral Sci. 120(4):369–372.

Bronckers AL, Guo J, Zandieh-Doulabi B, Bervoets TJ, Lyaruu DM, Li X, Wangemann P, DenBesten PK. 2011. Developmental expression of solute carrier family 26A member 4 (SLC26A4/pendrin) during amelogenesis in developing rodent teeth. Eur J Oral Sci. 119 Suppl 1:185–192.

Bronckers AL, Kalogeraki L, Jorna HJ, Wilke M, Bervoets TJ, Lyaruu DM, Zandieh-Doulabi B, DenBesten P, de Jonge H. 2010. The cystic fibrosis transmembrane conductance regulator (CFTR) is expressed in maturation stage ameloblasts, odontoblasts and bone cells. Bone. 46(4):1188–1196.

Claass A, Sommer M, de Jonge H, Kälin N, Tümmler B. 2000. Applicability of different antibodies for immunohistochemical localization of CFTR in sweat glands from healthy controls and from patients with cystic fibrosis. J Histochem Cytochem. 48(6):831–837.

Gawenis LR, Greeb JM, Prasad V, Grisham C, Sanford LP, Doetschman T, Andringa A, Miller ML, Shull GE. 2005. Impaired gastric acid secretion in mice with a targeted disruption of the NHE4 Na+/H+ exchanger. J Biol Chem. 280(13):12781–12789.

Guo J, Lyaruu DM, Takano Y, Gibson CW, DenBesten PK, Bronckers AL. 2015. Amelogenins as potential buffers during secretory-stage amelogenesis. J Dent Res. 94(3):412–420.

Höglund P, Haila S, Socha J, Tomaszewski L, Saarialho-Kere U, Karjalainen-Lindsberg ML, Airola K, Holmberg C, de la Chapelle A, Kere J. 1996. Mutations of the down-regulated in adenoma (DRA) gene cause congenital chloride diarrhoea. Nat Genet. 14 (3):316–319.

Jalali R, Guo J, Zandieh-Doulabi B, Bervoets TJ, Paine ML, Boron WF, Parker MD, Bijvelds MJ, Medina JF, DenBesten PK, et al. 2014. NBCe1 (SLC4A4) a potential pH regulator in enamel organ cells during enamel development in the mouse. Cell Tissue Res. 358(2):433–442.

Jiang Z, Asplin JR, Evan AP, Rajendran VM, Velazquez H, Nottoli TP, Binder HJ, Aronson PS. 2006. Calcium oxalate urolithiasis in mice lacking anion transporter Slc26a6. Nat Genet. 38(4):474–478.

Josephsen K, Takano Y, Frische S, Praetorius J, Nielsen S, Aoba T, Fejerskov O. 2010. Ion transporters in secretory and cyclically modulating ameloblasts: a new hypothesis for cellular control of preeruptive enamel maturation. Am J Physiol Cell Physiol. 299(6):C1299–C1307.

Ko SB, Shcheynikov N, Choi JY, Luo X, Ishibashi K, Thomas PJ, Kim JY, Kim KH, Lee MG, Naruse S, et al. 2002. A molecular mechanism for aberrant CFTR-dependent HCO_3^- transport in cystic fibrosis. EMBO J. 21(21):5662–5672.

Ko SB, Zeng W, Dorwart MR, Luo X, Kim KH, Millen L, Goto H, Naruse S, Soyombo A, Thomas PJ, et al. 2004. Gating of CFTR by the STAS domain of SLC26 transporters. Nat Cell Biol. 6(4):343–350.

Lacruz RS, Nanci A, Kurtz I, Wright JT, Paine ML. 2010. Regulation of pH during amelogenesis. Calcif Tissue Int. 86(2):91–103.

Lacruz RS, Nanci A, White SN, Wen X, Wang H, Zalzal SF, Luong VQ, Schuetter VL, Conti PS, Kurtz I, et al. 2010. The sodium bicarbonate cotransporter (NBCe1) is essential for normal development of mouse dentition. J Biol Chem. 285(32):24432–24438.

Lacruz RS, Smith CE, Moffatt P, Chang EH, Bromage TG, Bringas P Jr, Nanci A, Baniwal SK, Zabner J, Welsh MJ, et al. 2012. Requirements for ion and solute transport, and pH regulation during enamel maturation. J Cell Physiol. 227(4):1776–1785.

Lamprecht G, Gaco V, Turner JR, Natour D, Gregor M. 2009. Regulation of the intestinal anion exchanger DRA (downregulated in adenoma). Ann N Y Acad Sci. 1165:261–266.

Lohi H, Kujala M, Kerkelä E, Saarialho-Kere U, Kestilä M, Kere J. 2000. Mapping of five new putative anion transporter genes in human and characterization of SLC26A6, a candidate gene for pancreatic anion exchanger. Genomics. 70(1):102–112.

Lyaruu DM, Bronckers AL, Mulder L, Mardones P, Medina JF, Kellokumpu S, Oude Elferink RP, Everts V. 2008. The anion exchanger Ae2 is required for enamel maturation in mouse teeth. Matrix Biol. 27(2):119–127.

Paine ML, Snead ML, Wang HJ, Abuladze N, Pushkin A, Liu W, Kao LY, Wall SM, Kim YH, Kurtz I. 2008. Role of NBCe1 and AE2 in secretory ameloblasts. J Dent Res. 87(4):391–395.

Park HW, Nam JH, Kim JY, Namkung W, Yoon JS, Lee JS, Kim MK, Venglovecz V, Gray MA, Kim KH, et al. 2010. Dynamic regulation of CFTR bicarbonate permeability by [Cl-]i and its role in pancreatic bicarbonate secretion. Gastroenterology 139(2):620–631.

Ryu OH, Hu CC, Simmer JP. 1996. Comparative HPLC, SDS-PAGE, and immunoblot analyses of dental enamel proteins. Adv Dent Res. 10(2):150–158.

Sindic A, Chang MH, Mount DB, Romero MF. 2007. Renal physiology of SLC26 anion exchangers. Curr Opin Nephrol Hypertens. 16(5):484–490.

Smith CE. 1998. Cellular and chemical events during enamel maturation. Crit Rev Oral Biol Med. 9(2):128–161.

Smith CE, Chong DL, Bartlett JD, Margolis HC. 2005. Mineral acquisition rates in developing enamel on maxillary and mandibular incisors of rats and mice: implications to extracellular acid loading as apatite crystals mature. J Bone Miner Res. 20(2):240–249.

Soleimani M, Xu J. 2006. SLC26 chloride/base exchangers in the kidney in health and disease. Semin Nephrol. 26(5):375–385.

Song Y, Yamamoto A, Steward MC, Ko SB, Stewart AK, Soleimani M, Liu BC, Kondo T, Jin CX, Ishiguro H. 2012. Deletion of Slc26a6 alters the stoichiometry of apical Cl-/HCO-3 exchange in mouse pancreatic duct. Am J Physiol Cell Physiol. 303(8):C815–C824.

Steward MC, Ishiguro H. 2009. Molecular and cellular regulation of pancreatic duct cell function. Curr Opin Gastroenterol. 25(5):447–453.

Tizzano EF, Chitayat D, Buchwald M. 1993. Cell-specific localization of CFTR mRNA shows developmentally regulated expression in human fetal tissues. Hum Mol Genet. 2(3):219–224.

Trezise AE, Buchwald M. 1991. In vivo cell-specific expression of the cystic fibrosis transmembrane conductance regulator. Nature. 353(6343):434–437.

Wall SM, Hassell KA, Royaux IE, Green ED, Chang JY, Shipley GL, Verlander JW. 2003. Localization of pendrin in mouse kidney. Am J Physiol Renal Physiol. 284(1):F229–F241.

Wright JT, Hall KI, Grubb BR. 1996. Enamel mineral composition of normal and cystic fibrosis transgenic mice. Adv Dent Res. 10(2):270–274.

Xia W, Yu Q, Riederer B, Singh AK, Engelhardt R, Yeruva S, Song P, Tian DA, Soleiman M, Seidler U.2014. The distinct roles of anion transporters SLC26A3/Dra (DRA) and Slc26a6 (PAT-1) in fluid and electrolyte absorption in the murine small intestine. Pflugers Arch. 466(8):1541–1556.

Zeng W, Lee MG, Yan M, Diaz J, Benjamin I, Marino CR, Kopito R, Freedman S, Cotton C, Muallem S, et al. 1997. Immuno and functional characterization of CFTR in submandibular and pancreatic acinar and duct cells. Am J Physiol. 273(2 Pt 1):C442–C455.